two regions. While the seismic activity around Delhi region is mainly tectonic in nature, the same in the BEAS network region may have the additional influence of the loading of reservoirs in the region. Chaudhury and Srivastava[5] studied the reservoir-associated seismic activity around Bhakra, Pandoh and Pong dams in the study region. The increase in the seismic activity did not, however, bear any direct relationship with the reservoir level in the post-monsoon months. The region has also witnessed few earthquakes with foreshock–aftershock sequences, prominent among which is the Kinnaur earthquake of 19 January 1975 ($M_B = 6.2$) in which case the aftershocks continued for several years[5]. In view of the complexity of the region which is influenced by tectonically active Kangra region with foreshock–aftershock sequences as well as the activity in the vicinity of reservoirs, it is difficult to attribute these clusters to any particular phenomenon. It is, however, evident that both these phenomena strongly contribute to the temporal clusters observed in BEAS region. Better time resolution and detection capability of events would enable us to quantify these clusters in terms of the associated activity. Fractal approach to seismic clusters is thus an important tool to study and discriminate the temporal cluster of earthquakes under different seismogenic provinces. The method may also be extended to study the spatial cluster of events in a given tectonic set-up.

Temporal distribution of earthquakes in two distinct seismogenic provinces, viz. the BEAS and MOBILE network regions, has been studied using the fractal approach. The results suggest that the earthquake sequences in these regions differ significantly from the uniform distribution and are interpreted as a combination of scale-invariant clustering and random events. The BEAS network region exhibits relatively strong clustering ($D = 0.254$) in comparison to MOBILE network region ($D = 0.193$). The relatively strong clustering observed for BEAS events may be explained as due to the combined effect of tectonically active Kangra region characterized by foreshock–aftershock sequences and the seismic activity in the vicinity of reservoirs in the region.

1. Johnson, C., Keilis–Borok, V. I., Lamore, R. and Minster, B., *Computa. Seismol.*, 1984, **16**, 1–6.
2 De Natale, G. and Zollo, A., *Bull. Seismol. Soc. Am.*, 1986, **76**, 801–814
3 Mandelbrot, B , *Science*, 1967, **156**, 636–638.
4. Smalley, R. F. Jr., Chatelain, J. L., Turcotte, D. L. and Prevot, R., *Bull. Seismol. Soc. Am* , 1987, **77**, 1368–1381.
5. Chaudhury, H M. and Srivastava, H. N., Proceedings of Symposium on Earthquake Engineering, University of Roorkee, Roorkee, 1978, pp. 35–40.

ACKNOWLEDGEMENTS. We are grateful to the Director General, India Meteorology Department for permission to publish the paper.

One of the authors (RSD) is thankful to Secretary, Department of Science and Technology, New Delhi for encouragement.

Received 13 September 1993, revised accepted 5 April 1994

Localization of chromosome scaffold by transmitted- and incident-light fluorescence microscopy

Deepesh N. De and Rekha Ghosh

Agricultural Engineering Department, Indian Institute of Technology, Kharagpur 721 302, India

In order to demonstrate the chromosome scaffold the spermatocytes of a grasshopper were fixed in acetomethanol, treated with alkaline 2XSSC and stained with $AgNO_3$ solution. The air-dried preparations were fluorochromed with acridine orange (AO) and excited with either transmitted or incident beam of UV for fluorescence microscopic study. Under transmitted-light the scaffold is very clearly visible as non-fluorescent dark silver deposition along the middle of the chromosomes. However, under incident-illumination the scaffold is invisible and only the fluorescence of the epichromatin is observed. This indicates that the scaffold is situated longitudinally in the centre of a solid cylinder of epichromatin made of DNA-histone.

SINCE the early electron microscopic demonstration of a chromosome core surrounded by the epichromatin[1] and the existence of a proteinaceous scaffold surrounded by DNA loops[2], Howell and Hsu[3] were able to demonstrate a chromosome core at the light microscopic level by developing a silver-deposition technique. Since then a number of authors[4–7] confirmed the presence of such a scaffold. The scaffold is thought to be involved in chiasma-formation[8] and is possibly bipartite in nature[9] and is a permanent component of the chromosomes[10]. After complete removal of histones from the metaphase chromosomes, a very limited set of proteins remains in the scaffold and the enzyme topoisomerase II is one of them[11]. The enzyme topo II provides a structural anchorage for the chromatin loops to the axial scaffold of the chromosomes[12, 13]. The anchorage or the scaffold attachment region (SAR) of DNA is characterized by A-T rich consensus sequence[14]. On the other hand the catalytic activity of topo II in facilitating the strand passage is intimately associated with chromosome condensation as has been demonstrated by a cytological analysis of appropriate mutants in fission yeast[15] and from *in vitro* studies of cell extracts[16]. The present transmitted- and incident-light fluorescence microscopic study of the silver-stained scaffold shows that it is centrally located inside the epichromatin during the

various stages of meiosis of a grasshopper *Acrida turrita*.

The testicular follicles of *Acrida turrita* were dissected out in 0.075 M KCl, fixed in aceto-methanol, minced and squashed. After removal of the cover glass, the air-dried slides were treated for 1.5 min in 0.01 N NaOH in 2XSSC[4]. After staining with silver-nitrate[17], the air-dried slides were fluorochromed with AO[18]. The preparations were observed with the aid of a Carl Zeiss Jena Fluoval fluorescence microscope which permits convenient observation and photomicrography of the same specimen in white light-bright field, transmitted- and incident-light excitation in quick succession. The BG 12/4 mm excitation filter provided the peak transmission at about 400 nm and the OG 1/1 barrier filter G-249 permitted transmission above 546 nm.

Due to the staining with AO, chromatin components and chromosomes appeared yellow under white light. The silver-staining was evident as dark grains or black deposits on various parts of nuclei and chromosomes and the deposition pattern was found to be highly reproducible. The interphase and leptotene nuclei did not show any silver deposition, except at certain points which are heterochromatic. In these stages the proteinaceous scaffold is too lax and tenuous to produce any significant deposition of silver grain. Under white light the scaffold appears as a fine deep brown strand running along the middle of the zygotene chromosomes (Figure 1). The centromeric as well as intercalary heterochromatin appear as pairs of dark spots placed on the scaffold. The chromosomes at diakinesis (Figure 3 *a*) and metaphase I (Figure 2 *a*) show clearly a black scaffold surrounded by yellow coloured epichromatin. As the chromosome condenses further the deposition on the scaffold becomes heavier. Thus the highly condensed anaphase II chromosomes appear to be completely covered with silver deposits (Figure 4 *a*). When the same preparations were viewed under transmitted-light fluorescence microscopy, the scaffold appeared dark surrounded by orange-red fluorescence of epichromatin (Figures 2 *b* and 3 *b*). The epichromatin is monitored by the fluorescence of the chromophore acridine orange which is excited by the UV illumination of the microscope. The epichromatin contains DNA which is denatured by alkaline SSC treatment and is devoid of histones due to aceto-methanol fixation and subsequent squashing in acetic acid. Under transmitted-light, the chromosomes at anaphase II appear as very dark masses surrounded by a thin halo of red fluorescence (Figure 4 *b*). In these chromosomes, the scaffold has undergone intense compaction along with most of the epichromatin and only a part of surface DNA is exposed to produce AO fluorescence. When the same preparations are viewed with incident-light excitation, the appearance is strikingly different. The diakinesis chromosomes appear uniformly orange indicative of denatured DNA and the scaffold is totally invisible (Figure 3 *c*). Similar is the appearance of the chromosomes at all the later stages (Figures 2 *c* and 4 *c*). In other words, with the aid of epiillumination the scaffold is not at all visible, even at anaphase II where the scaffold is very thick. The appearance is due to the fluorescence of epichromatin DNA which is external to the scaffold.

The difference in appearance of the same chromosomes under two types of illumination is due to the fact that under transmitted-light excitation, the emission from the epichromatin stained with AO is obstructed by the Ag grains deposited at the scaffold and those on the top of the scaffold are not illuminated at all. Thus the scaffold stands out very clearly surrounded by the epichromatin (Figure 5 *a*). In contrast, the incident light from above excites the epichromatin which fluoresces uniformly and the scaffold remains hidden inside (Figure 5 *b*). In this case, the scaffold which is surrounded by the epichromatin is not interfering. If the chromosomes were flat or plate-like, the scaffold should have been visible under epiillumination. In a previous study we have shown that the scaffold is a permanent structure[10]. By the present method, the scaffold can be distinctly traced from zygotene onwards and as the meiosis proceeds the scaffold undergoes condensation parallel to the condensation of the chromosome. This parallelism is in consonance with the fact that topo II is a major component of the scaffold and it plays a vital role in condensation. The most dramatic demonstration of the scaffold and the epichromatin is seen in anaphase II chromosomes where the heavily silver-deposited scaffold is surrounded by the halo of AO-fluorescing epichromatin. This also indicates that while most of

Figures 1–4. Meiotic chromosomes after silver-staining followed by fluorochroming with acridine orange. The series a, b, c of each figure was photographed from the same final preparation, without any subsequent change or processing, under bright field microscopy with white light, under transmitted-excitation and incident-excitation fluorescence respectively, in succession. Bar represents 10 μm for all photomicrographs **1**. The zygotene nucleus shows fine deep brown scaffold (thin arrow) and dark paired dots of heterochromatin (thick arrow) Epichromatin is light brown **2** *a*, Under bright field the metaphase I shows 11 bivalents and single X chromosome, each with a thick distinct black scaffold connected with the heterochromatic blocks The brown epichromatin surrounds the scaffold **2** *b*, Under transmitted-excitation the scaffold is dark brown with the epichromatin fluorescing red **2** *c*, Under incident-excitation no scaffold is visible, only epichromatin fluoresces. **3** *a*, At diakinesis the brown thick scaffold is distinguishable from the heavily deposited terminal and intercalary heterochromatin **3** *b*, Transmitted-excitation exhibits the scaffold very distinctly and the epichromatin appears orange-red **3** *c*, Under epiillumination the scaffold remains invisible and only epichromatin fluoresces orange **4** *a*, Anaphase II scaffold is thick and black due to heavy deposition of silver and epichromatin is not visible **4** *b*, Transmitted-excitation shows an orange-red halo (arrow) around the chromosomes indicating the presence of a thin layer of epichromatin surrounding the thick scaffold **4** *c*, With incident-excitation, epichromatin fluoresces and scaffold is invisible →

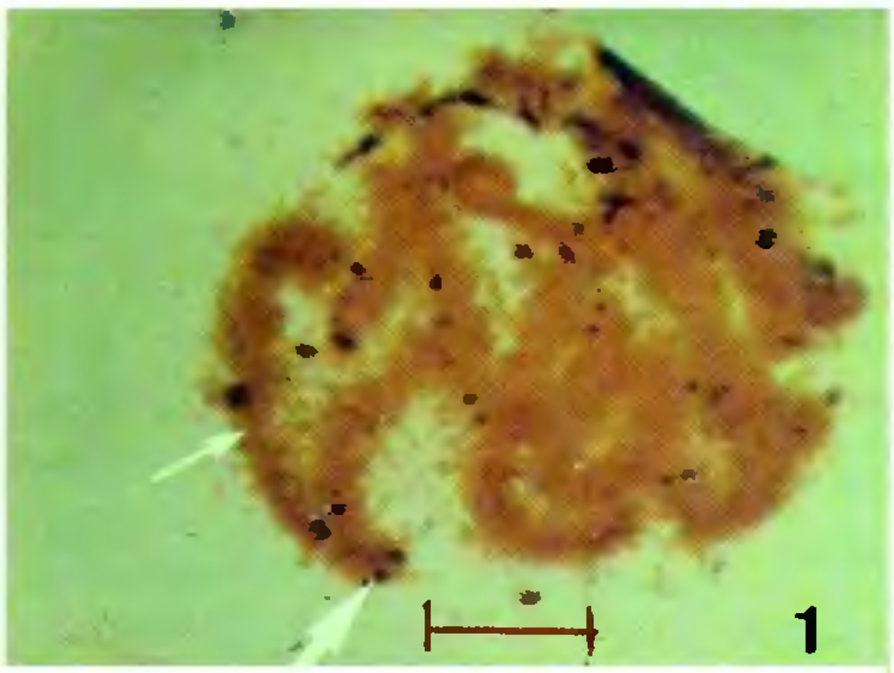
1

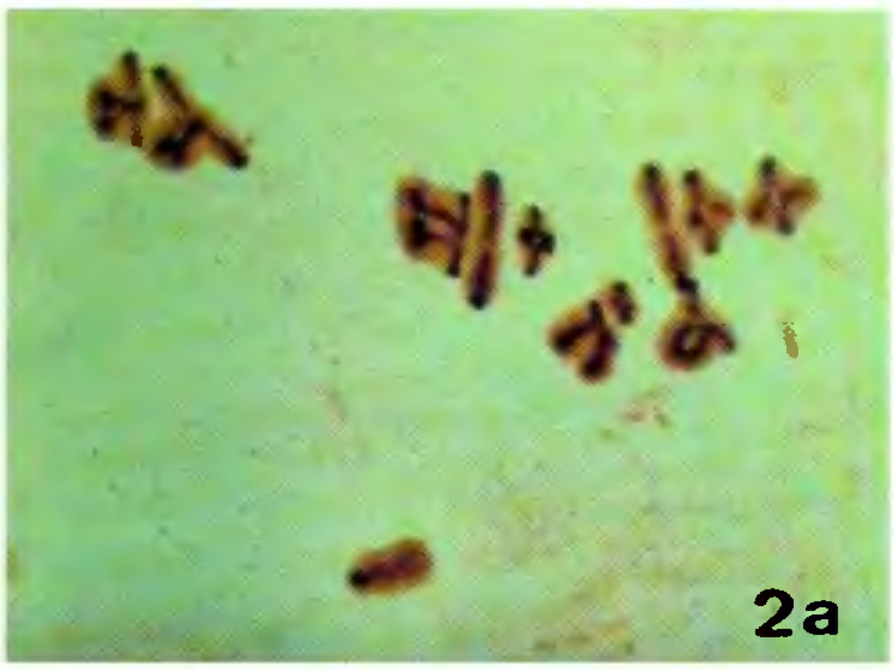
2a

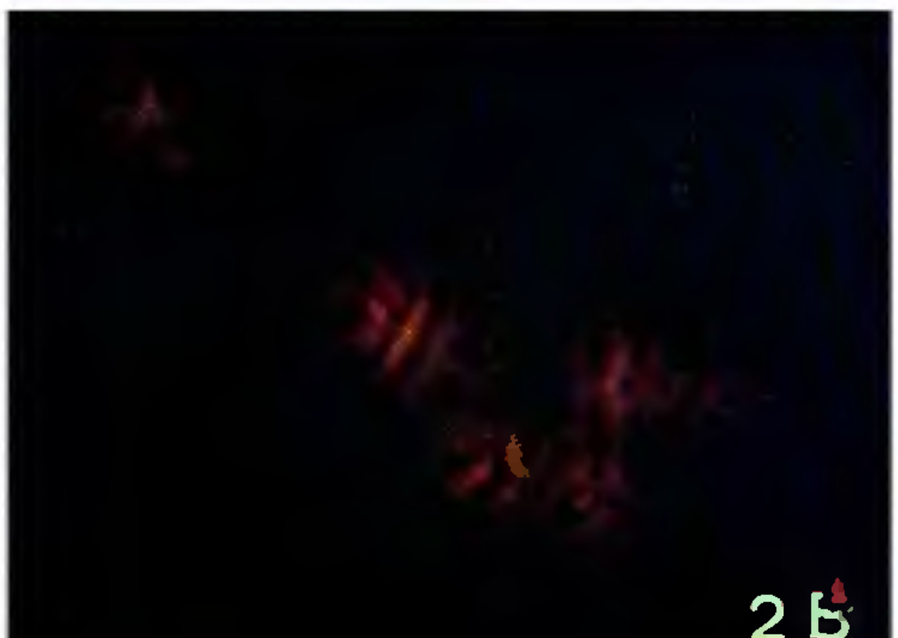
2 b

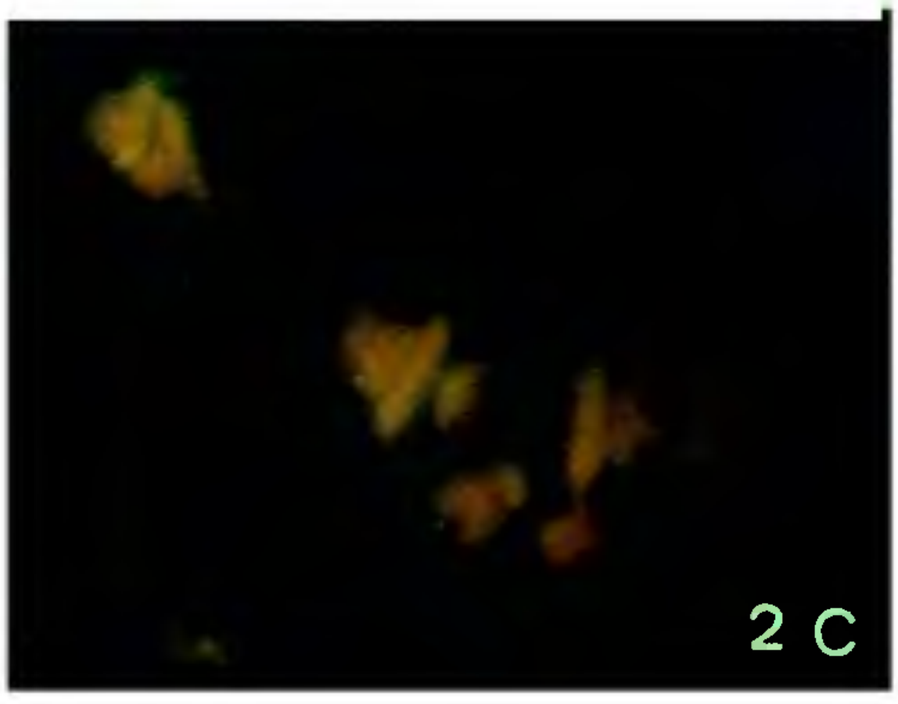
2 C


3a

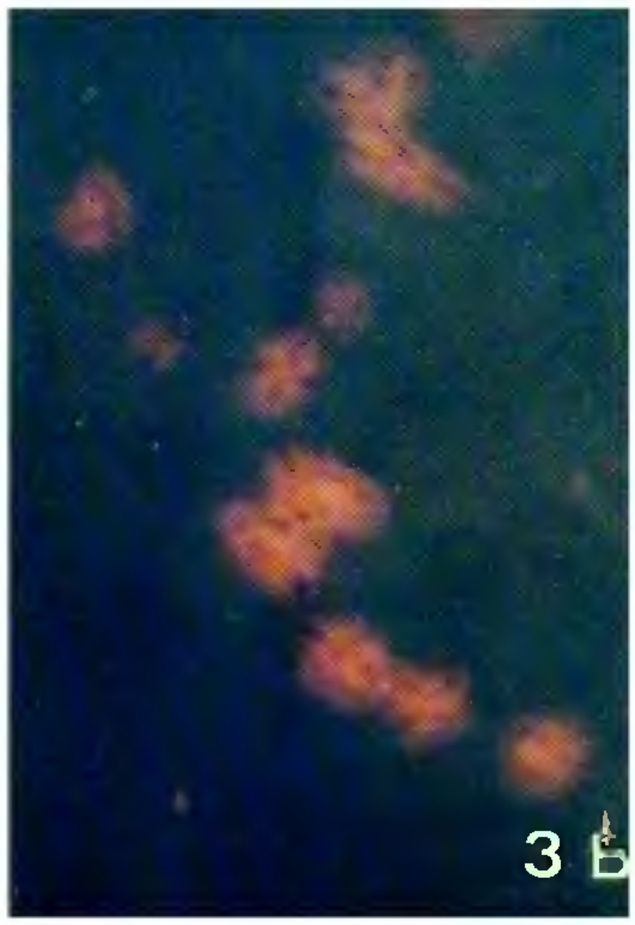
3 b


3 C


4a


4 b


4 C

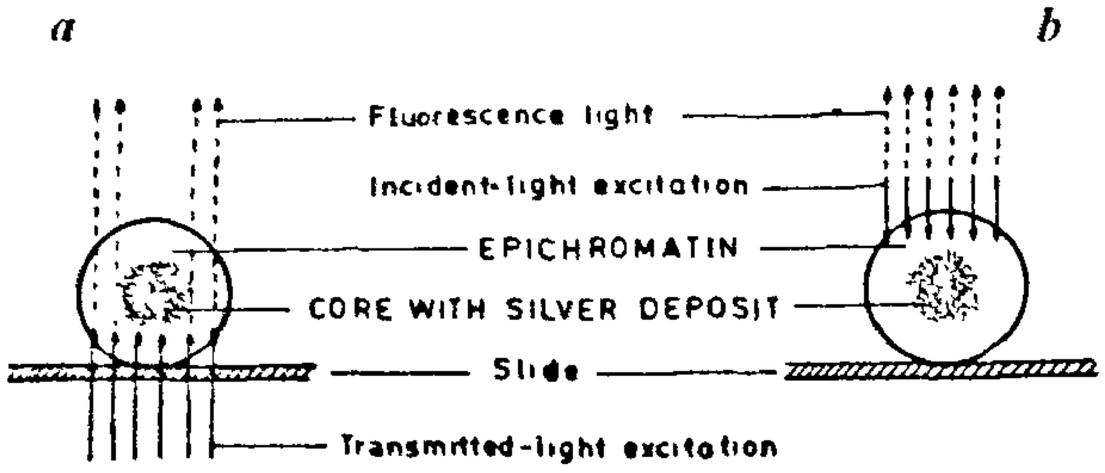

Figures 5. Diagrammatic representation of fluorescence from the cross-section of a silver-stained chromosome by two types of excitation *a*. In transmitted-light excitation, the silver deposition of the scaffold hinders the fluorescence light emitted by the epichromatin situated immediately above the scaffold making it visible *b*. In incident-light excitation, only the fluorescence light emitted by the epichromatin is visible and the scaffold remains invisible since it does not come in the way of either the incident or the fluorescence beam

chromatin fibres are possibly wrapped up by the scaffold protein, a portion of the chromatin remains exposed to the nucleoplasm. This may be equivalent to what Rattner[19] calls as the surface domain. Similarly the proteins of the scaffold along with SAR belong to the central domain. Thus it is concluded that the proteinaceous scaffold is situated longitudinally along the centre of the solid cylinder of epichromatin made of DNA-histone during all stages of chromosome cycle.

1 Stubblefield, E and Wray, W, *Chromosome*, 1971, **32**, 262–294
2 Paulson, J R and Laemmli, U K, *Cell*, 1977, **12**, 817–828
3 Howell, W M and Hsu, T C., *Chromosoma*, 1979, **79**, 61–66
4 Satya-Prakash, K L, Hsu, T C and Pathak, S, *Chromosoma*, 1980, **81**, 1–8
5 Rufas, J S, Gimenez-Martin, G. and Esponda, P, *Cell Biol Int Rep*, 1982, **6**, 261–267
6 Sentis, C, Rodriguez-Campos, A, Stockert, J C and Fernandez-Piqueras, J, *Chromosoma*, 1984, **10**, 317–321
7 Nokkala, S, *Hereditas* 1985, **103**, 111–117.
8 Santos, J L Lopez, G and Lacadena, J R, *Genome*, 1987, **29**, 235–238
9 Zhao, F, Hao, S and Xing, M, *Chromosoma*, 1991, **100**, 323–329
10 Ghosh, R and De, D N, *Caryologia*, 1994, **47**, 59–64
11 Earnshaw, W C., Halligan, B, Cooke, C. A, Heck, M M S and Liu, L. F, *J Cell Biol*, 1985, **100**, 1706–1715.
12 Mirkovitch, J, Mirault, M F and Laemmli, U K, *Cell*, 1984, **39**, 223–232
13 Kas, E and Laemmli, U K, *EMBO J*, 1992, **11**, 705–746
14 Gasser, S M, Amati, B B, Cardenas, M E and Hofmann, J F X, *Int Rev Cytol*, 1989, **119**, 57–96
15 Uemura, T, Ohkura, H, Adachi, Y, Morino, K, Shiozaki, K and Yanagida, M, *Cell*, 1987, **50**, 917–925
16 Adachi, Y, Luke, M and Laemmli, U K, *Cell*, 1991, **64**, 137–148
17 Pathak, S and Elder F F B, *Hum Genet*, 1980, **54**, 171–175
18 Bertalanffy, L Von, *Protoplasma*, 1963, **57**, 51–83
19 Rattner, J B, *Chromosoma*, 1992, **101**, 259–264

ACKNOWLEDGEMENT We thank Professor Pradyot Bhanja of Burdwan University for his advice on instrumentation

Received 7 June 1993 revised accepted 25 May 1994

Evaluation of growth behaviour of deodar and blue pine by using tree ring data from Uttarkashi, UP Himalaya

R. R. Yadav and A. Bhattacharyya

Birbal Sahni Institute of Palaeobotany, 53 University Road, Lucknow 226 007, India

The present study deals with the harmonic analysis of ring width series of deodar (1788–1987 AD) and blue pine trees (1826–1988) growing in Uttarkashi, UP Himalaya to understand short term fluctuations in productivity. Approximation of these tree ring series showed very good synchronization with cross correlation, 0.826 for *C. deodara* and 0.919 for *P. wallichiana*. Prediction of the series for 15 years by using this model indicated high values of similarity coefficient between predicted and original index values (64% for *C. deodara* and 71.4% for *P. wallichiana*). The results indicate that the dendrochronological series from the Himalayan regions could be used for short range predictions of tree growth.

FLUCTUATIONS in widths of tree ring sequences reflect the dynamics of wood growth dependent on environmental variables. It has been noted by several workers[1–9] that variations in tree ring widths differing in amplitude and duration are repeated more or less regularly over time. The cyclic components present in the tree ring time series have been used by several workers[9–14] for the prediction of the series to understand tree growth dynamics. Such predictions of the dendrochronological series would be useful in sustainable forest resource management.

In India variety of tree species growing in tropical and temperate regions are known to produce distinct growth rings. Studies so far conducted on some tree species from both the regions using ring width[15–21] and isotopic[22–24] variations have shown good dendroclimatic potential. With the development of the subject, besides its application in climatic studies variations in tree ring features such as thickness, density and chemical compositions have shown promise to assess how forests or individual trees respond to atmospheric chemistry, management and many other forest disturbances[25–29]. Application of such studies in various forestry aspects